



Electric-field and strain effect on magnetism on transition metal dichalcogenides

Munkhsaikhan Gonchigsuren^{1†}, Odkhuu Dorj²

¹ *Department of Physics, School of Applied Sciences, Mongolian University of Science and Technology, Ulaanbaatar, Mongolia*

² *Department of Physics, the College of Natural Sciences, Incheon National University, Korea*

ABSTRACT. Herein, from first-principles density functional calculations, intrinsic magnetism and magnetocrystalline anisotropy (MA) in two-dimensional (2D) structure and individual atom pairs are shown effectively controllable by means of simultaneous voltage and strain effects. By tuning the strain in transition metal dichalcogenides (TMDs) MoS₂, WS₂, MoSe₂ and WSe₂ with Os adatom as a model system, we demonstrate that the voltage dependence of MA varies from an extremely large value of 150 meV/Os in perpendicular to the lateral plane into -25 meV/Os in plane by an electric field of only 0.1–0.2 V/Å.

KEYWORDS. Magnetic momentum, 2D materials, first principles calculation

1. INTRODUCTION

Single molecule or atomic magnets deposited on two dimensional (2D) or ultrathin-film structures exhibit an atomic-scale upper limit of magnetocrystalline anisotropy (MA), in addition to their small size and intrinsic magnetism, which would qualify for today's demand to maximize the information storage density in magnetic memories [1–3]. In particular, large perpendicular MA (PMA) is of crucial significance for the stable long-term magnetic random access memory (MRAM) and spin-transfer torque memory (STT-RAM) [4–6]. Recently, researchers have focused on individual transition metal (TM) magnets, including Fe, Co, and Mn, deposited onto 2D (mainly graphene and TM dichalcogenides) and thin-film surfaces (Pt, CuN, and MgO) [7–11]. For example, an extremely large PMA up to an order of 100 meV has been first predicted in cobalt dimer-benzene pairs [7]. In subsequent experiments, large PMA values of 9 and 60 meV have been achieved in individual Co atoms on Pt(111) [8] and MgO(001) [9], respectively. More remarkably, Ru and Os magnets, which are isoelectronic to Fe, have been identified to exhibit even larger PMA up to 60-200 meV when placed on MoS₂ [12] and MgO(001) [13]. Beyond these atomic-scale PMA, more recent development of memory technologies requires a breakthrough that leads to the complete electric-field switching of magnetization direction in the absence of the magnetic field or STT current [14–16].

Received: 02 November 2021 / Revised: 22 November 2021 / Accepted: 22 December 2021

†Corresponding author's email: gmunkhsaikhan@must.edu.mn

2. COMPUTATIONAL METHODS

We employed density functional theory (DFT) calculations as implemented in the Vienna ab initio simulation package (VASP) [17]. The generalized gradient approximation (GGA), parameterized by Perdew, Burke, and Ernzerhof (PBE), is used to describe the exchange correlation functional [18]. Figure 1(a) shows a 3×3 supercell structure of MoS₂ monolayer. Our model consists of a single Os atom embedded into a monosulfur vacancy in 3×3 MoS₂, as schematically illustrated in Figure 1(b), which is energetically favorable [12]. Such an intrinsic defect of a sulfur vacancy occurs quite often during the sample growth [19, 20]. A vacuum no less than 15\AA is used to separate the periodic slabs along the z axis. Energy cutoff of 500 eV, $11 \times 11 \times 11$ k -point mesh, and relaxation force criterion of 10^{-2} eV/ \AA were adopted for the structure optimization. MA energy (MAE) is obtained based on the total energy difference when the magnetization directions are in the xy plane (E^{\parallel}) and along the z axis (E^{\perp}), $MAE = E^{\parallel} - E^{\perp}$. We imposed a denser k -point mesh of $21 \times 21 \times 1$ in noncollinear calculations, which is sufficient to obtain well converged MAE. The spin-orbit coupling (SOC) term is included in a second-variational way employing scalar relativistic calculations of the valence state [21].

3. RESULTS AND DISCUSSION

As often occurs in 2D structures, a significant amount of biaxial strain up to 2.5% is tolerated in TMD monolayer, due to the lattice mismatch with an underlying substrate [22–24]. We first investigate the effect of the biaxial strain on the zero-field intrinsic orbital magnetic moment (μ_0) and MAE of the Os $5d$ orbitals on MoS₂ in Figures 1(c) and 1(d), respectively. Both the compressive and tensile strains (η) up to $\pm 4\%$ are imposed into the 2D lattice of MoS₂, where $\eta = \frac{(a_{\parallel} - a_0)}{a_0} \times 100\%$, and a_{\parallel} and a_0 are the variable and equilibrium lattice constants, respectively. The optimized lattice constant of the pristine MoS₂ monolayer is 3.18\AA , which in an experiment is 3.15\AA [25]. The lattice constant remains unchanged upon the S-site Os adsorption. While μ_0 projected on the xy plane (μ_0^{\parallel}) does not alter much under strain, the strain has dramatic effect on μ_0 along the z axis (μ_0^{\perp}) (Figure 1(c)). Here, we recall that MAE of the Os adatom on MoS₂ at zero strain is 102 meV/Os [12]. Positive MAE stands for the preferable direction of magnetization normal to MoS₂ plane, i.e., PMA. This large PMA is associated with the strong bipyramidal crystal field effects in the low-spin state (LS) complex, through the strong band overlaps between the Os $5d$ and Mo $4d$ orbitals [12]. Practically, the atomic-scale PMA up to 60 meV/atom have been already achieved in individual $3d$ Co, Fe, and Mn atoms [8–11]. These experiments support our prediction of practical $5d$ -based PMA at the atom length scale. We further find from Figure 1(d) that the strain has a large impact on PMA, where MAE increases up to 140 meV/Os at $\eta = -4\%$ (compressive strain) and decreases to 32 meV/Os at $\eta = 4\%$ (tensile strain). This is consistent with the orbital moment trend indicated in Figure 1(c), obeying the Bruno rule.

Bader charge analyses indicate that the Os $5d^6$ orbitals accumulate an extra charge of $0.3e$ from its surrounding Mo atoms as Os has larger electronegativity (2.20) than Mo (2.16). The captured electrons occupy the high-lying a_1 and e' levels, leading to unpaired

electrons in the LS state. From $S = 1/2$, one can formulate the effective magnetic moment (μ_{eff}) of $1.73\mu_B$ in the LS complex, according to the spin-only formula $\mu_{\text{eff}} = \sqrt{n(n+2)}\mu_B$, where n is the number of unpaired electrons. This spin-only magnetic moment is almost reproduced in our self-consistent calculations ($1.59\mu_B$). Furthermore, the spin magnetic moment (μ_s) decreases from $1.64\mu_B$ at $\eta = -4\%$ to $1.45\mu_B$ at $\eta = 4\%$. As the Os-Mo interlayer distance (d) decreases from 1.92 \AA (at $\eta = -4\%$) to 1.64 \AA (at $\eta = 4\%$), the Os adatom further gains a more charge of $0.2e$ at $\eta = 4\%$ compared with $\eta = -4\%$. This charge transfer occurs mainly in the minority-spin state, which in turn reduces μ_s under compressive \rightarrow tensile strain.

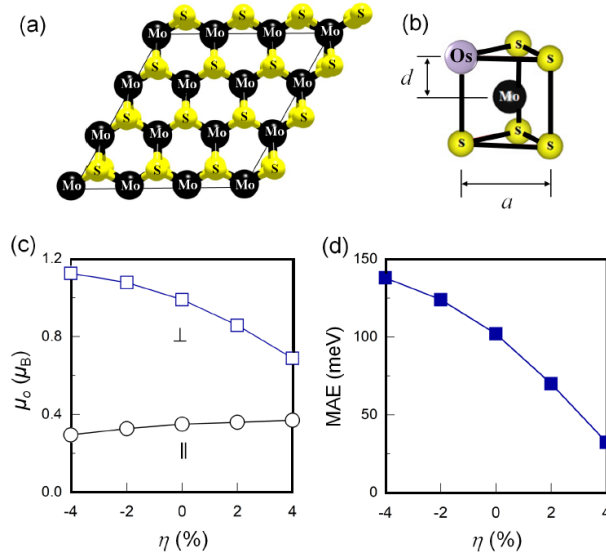


FIGURE 1. (a) Top view of a 3×3 supercell structure of MoS₂ monolayer. The larger black and smaller yellow spheres represent the Mo and S atoms, respectively. (b) Schematic diagram representing a monosulfur vacancy in which the Os adatom is embedded. (c) Orbital magnetic moments μ_0 , along the z axis and on the xy plane, and (d) magnetic anisotropy energy MAE of the Os adatom on MoS₂ with a monosulfur vacancy for different strains η .

In addition to the strain effect, we now explore the effect of an external electric field on the intrinsic magnetism. We show in Figures 2(a) and 2(b) the voltage dependence of the strain controlled μ_s and MAE of the Os adatom on MoS₂, respectively. The external electric field \vec{E}_{ext} is oriented normal to the planar sheet, where the upward direction pointing toward the Os-free sulfur plane represents the positive field. The dipole correction was taken into account to eliminate an artificial field across the unit cell imposed by the periodic boundary condition.

Here, the effective electric field is defined as $\vec{E}_{\text{eff}} = \frac{\vec{E}_{\text{ext}}}{\epsilon^\perp}$, where ϵ^\perp is the out-of-plane component of the dielectric tensor of MoS₂. We find that ϵ^\perp values of the pristine MoS₂ monolayer with $\eta = -4, -2, 0, 2, \text{ and } 4\%$ are 3.76, 3.60, 3.48, 3.35, and 3.25, respectively.

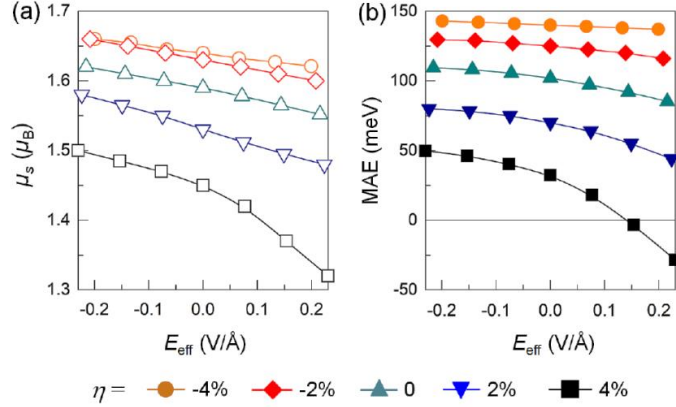


FIGURE 2. (a) Spin magnetic moment μ_s and (b) magnetic anisotropy energy MAE of the Os adatom on MoS₂ a monosulfur vacancy as function of the effective electric field \vec{E}_{eff} for different strains η .

Both μ_s and MAE decrease as E_{eff} reverses from negative to positive, in a similar trend with μ_0^\perp (not shown). In particular, the voltage-controlled μ_s and MAE are more depressed by the tensile strain than the compressive strain. At $\eta = 4\%$, the negative→positive field enhances the charge of the Os-5*d* orbitals from 6.35 *e* (at $E_{\text{eff}} = -0.23\text{V}/\text{\AA}$) to 6.51 *e* (at $E_{\text{eff}} = 0.23\text{V}/\text{\AA}$). This extra charge is accumulated mainly in the minority spin *a*1 state, as discussed in the following paragraph, which reduces the spin moment. Interestingly, at $\eta = 4\%$, PMA undergoes a transition to an in-plane magnetization when $E_{\text{eff}} = -0.15\text{V}/\text{\AA}$. Such electric control of magnetization reorientation of the atomic-scale PMA is exceptionally uncommon, which, if ever realized, holds promise for future applications in magnetoelectric memories.

Results from calculations on strain effect on magnetism of MoS₂, WS₂, MoSe₂ and WSe₂ with Os adatom is presented in Tables 1 to 4. Here, ground state energy, lattice parameters, magnetic momentum and ... $\eta = -4, -2, 0, 2, \text{ and } 4\%$ are found, respectively.

TABLE 1. MoS₂: Strain effect on magnetism

System	Strain, η				
	-4	-2	0	2	4
Mo ₉ S ₁₇ Os ₁					
E_0 (eV)	-195.9	-196.9	-197.2	-196.9	-196.2
H_f (eV/atom)	-0.17	-0.18	-0.19	-0.2	-0.21
<i>a</i> and <i>b</i> (Å)	9.16	9.35	9.54	9.73	9.92
MM - total (μ_B)	1.807	1.798	1.779	1.763	1.731
Ku (meV)	138.51	128.86	103.36	70.01	36.07

TABLE 2. MoSe₂: Strain effect on magnetism

System	Strain, η				
	-4	-2	0	2	4
Mo ₉ Se ₁₇ Os ₁	-4	-2	0	2	4
E ₀ (eV)	-180.5	-181.3	-181.6	-181.3	-180.6
H _f (eV/atom)	-0.18	-0.19	-0.20	-0.21	-0.22
a and b (Å)	9.55	9.75	9.94	10.14	10.34
MM - total (μ_B)	1.82	1.79	1.78	1.78	1.77
Ku (meV)	73.1	-57.0	-52.0	-44.7	-32.5

TABLE 3. WS₂: Strain effect on magnetism

System	Strain, η				
	-4	-2	0	2	4
W ₉ S ₁₇ Os ₁	-4	-2	0	2	4
E ₀ (eV)	-213.1	-214.1	-214.4	-214.1	-213.3
H _f (eV/atom)	-0.14	-0.15	-0.16	-0.17	-0.18
a and b (Å)	9.17	9.36	9.55	9.74	9.93
MM - total (μ_B)	1.797	1.776	1.754	1.732	1.723
Ku (meV)	121.48	110.86	80.08	38.45	-12.05

TABLE 3. WSe₂: Strain effect on magnetism

System	Strain, η				
	-4	-2	0	2	4
W ₉ Se ₁₇ Os ₁	-4	-2	0	2	4
E ₀ (eV)	-195.8	-196.7	-197.0	-196.7	-195.9
H _f (eV/atom)	-0.19	-0.20	-0.21	-0.22	-0.23
a and b (Å)	9.55	9.75	9.95	10.15	10.35
MM - total (μ_B)	1.79	1.75	1.74	1.74	1.73
Ku (meV)	35.7	-45.8	-42.8	-35.2	-26.0

4. CONCLUSIONS

In conclusion, using first-principles density functional calculations, we have demonstrated an extremely large PMA. More importantly, such a giant PMA has been further predicted to reverse into in-plane magnetization by tuning the voltage and strain effects. The present results provide a viable route to achieving atomic-scale magnetic anisotropy and its magnetization reversal by exploiting the voltage and strain engineering in 2D structures, opening interesting prospects in two-dimensional magnetoelectric spintronics.

Acknowledgments

This work was financially supported by the Science Technology Foundation Project ("Studies of the fabrication of nanostructured WSe₂ and MoSe₂" ShUS-2019/08) of Mongolia.

REFERENCES

- [1] A. A. Khajetoorians, J. Wiebe, B. Chilian, and R. Wiesendanger, *Realizing all-spin-based logicoperations atom by atom*, *Science* **332**, 1062 (2011).
- [2] A. A. Khajetoorians, B. Baxevanis, C. Hubner, T. Schlenk, S. Krause, T. O. Wehling, S. Lounis, A. Lichtenstein, D. Pfannkuche, J. Wiebe, and R. Wiesendanger, *Current-driven spin dynamics of artificially constructed quantum magnets*, *Science* **339**, 55 (2013).
- [3] A. A. Khajetoorians and J. Wiebe, *Science* **344**, 976 (2014).

- [4] J. C. Slonczewski, Conductance and exchange coupling of two ferromagnets separated by a tunneling barrier, *Phys. Rev. B* **39**, 6995 (1989).
- [5] S. Ikeda, K. Miura, H. Yamamoto, K. Mizunuma, H. D. Gan, M. Endo, S. Kanai, J. Hayakawa, F. Matsukura, and H. Ohno, *A perpendicular-anisotropy CoFeB-MgO magnetic tunnel junction*, *Nat. Mater.* **9**, 721 (2010).
- [6] A. D. Kent, Perpendicular all the way, *Nat. Mater.* **9**, 699 (2010).
- [7] R. Xiao, D. Fritsch, M. D. Kuz'min, K. Koepf, H. Eschrig, M. Richter, K. Vietze, and G. Seifert, *Co Dimers on Hexagonal Carbon Rings Proposed As Subnanometer Magnetic Storage Bits*, *Phys. Rev. Lett.* **103**, 187201 (2009).
- [8] P. Gambardella, S. Rusponi, M. Veronese, S. S. Dhesi, C. Grazioli, A. Dallmeyer, I. Cabria, R. Zeller, P. H. Dederichs, K. Kern, C. Carbone, and H. Brune, *Giant Magnetic Anisotropy of Single Cobalt Atoms and Nanoparticles*, *Science* **300**, 1130 (2003).
- [9] I. G. Rau, S. Baumann, S. Rusponi, F. Donati, S. Stepanow, L. Gragnaniello, J. Dreiser, C. Piamonteze, F. Nolting, S. Gangopadhyay, O. R. Albertini, R. M. Macfarlane, C. P. Lutz, B. A. Jones, P. Gambardella, A. J. Heinrich, and H. Brune, *Reaching the magnetic anisotropy limit of a 3d metal atom*, *Science* **344**, 988 (2014).
- [10] F. Donati, L. Gragnaniello, A. Cavallin, F. D. Natterer, Q. Dubout, M. Pivetta, F. Patthey, J. Dreiser, C. Piamonteze, S. Rusponi, and H. Brune, *Tailoring the Magnetism of Co Atoms on Graphene through Substrate Hybridization*, *Phys. Rev. Lett.* **113**, 177201 (2014).
- [11] C. F. Hirjibehedin, C.-Y. Lin, A. F. Otte, M. Ternes, C. P. Lutz, B. A. Jones, and A. J. Heinrich, *Large Magnetic Anisotropy of a Single Atomic Spin Embedded in a Surface Molecular Network*, *Science* **317**, 1199 (2007).
- [12] D. Odkhuu, Giant perpendicular magnetic anisotropy of an individual atom on two-dimensional transition metal dichalcogenides, *Phys. Rev. B* **94**, 060403(R) (2016).
- [13] X. Ou, H. Wang, F. Fan, Z. Li, and H. Wu, *Giant Magnetic Anisotropy of Co, Ru, and Os Adatoms on MgO (001) Surface*, *Phys. Rev. Lett.* **115**, 257201 (2015).
- [14] W. Eerenstein, N. D. Mathur, and J. F. Scott, *Multiferroic and magnetoelectric materials*, *Nature* **442**, 759 (2006).
- [15] M. Bibes and A. Barthelemy, *Towards a magnetoelectric memory*, *Nat. Mater.* **7**, 425 (2008).
- [16] N. Spaldin, S. W. Cheong, and R. Ramesh, *Multiferroics: Past, present, and future*, *Phys. Today* **63**, 38 (2010).
- [17] G. Kresse and J. Hafner, *Ab initio molecular dynamics for liquid metals*, *Phys. Rev. B* **47**, 558 (1993).
- [18] J. Perdew, K. Burke, and M. Ernzerhof, *Generalized Gradient Approximation Made Simple*, *Phys. Rev. Lett.* **77**, 3865 (1996).
- [19] W. Zhou, X. Zou, S. Najmaei, Z. Liu, Y. Shi, J. Kong, J. Lou, P. M. Ajayan, B. I. Yakobson, and J. C. Idrobo, *Intrinsic structural defects in monolayer molybdenum disulfide*, *Nano Lett.* **13**, 2615 (2013).
- [20] H. Li, C. Tsai, A. L. Koh, L. Cai, A. Contryman, A. H. Fragapane, J. Zhao, H. S. Han, H. C. Manoharan, F. Abild-Pedersen, J. K. Nørskov, and X. Zheng, *Activating and optimizing MoS₂ basal planes for hydrogen evolution through the formation of strained sulphur vacancies*, *Nat. Mater.* **15**, 48 (2016).
- [21] D. D. Koelling and B. N. Harmon, *J. Phys. C Solid State* **10**, 3107 (1977).
- [22] A. C. Gomez, R. Roldan, E. Cappelluti, M. Buscema, F. Guinea, H. S. J. van der Zant, and G. A. Steele, *Local Strain Engineering in Atomically Thin MoS₂*, *Nano Lett.* **13**, 5361 (2013).
- [23] C. R. Zhu, G. Wang, B. L. Liu, X. Marie, X. F. Qiao, X. Zhang, X. X. Wu, H. Fan, P. H. Tan, T. Amand, and B. Urbaszek, *Strain tuning of optical emission energy and polarization in monolayer and bilayer MoS₂*, *Phys. Rev. B* **88**, 121301 (2013).
- [24] H. Li, A. W. Contryman, X. Qian, S. M. Ardakani, Y. Gong, X. Wang, J. M. Weisse, C. H. Lee, J. Zhao, P. M. Ajayan, J. Li, H. C. Manoharan, and X. Zheng, *Optoelectronic crystal of artificial atoms in strain-textured molybdenum disulphide*, *Nat. Commun.* **6**, 7381 (2015).
- [25] N. Wakabayashi, H. G. Smith, and R. M. Nicklow, *Lattice dynamics of hexagonal MoS₂ studied by neutron scattering*, *Phys. Rev. B* **12**, 659 (1975).



This article is an open access article distributed under the terms and conditions of the Creative Commons Attribution (CC BY) license (<https://creativecommons.org/licenses/by/4.0/>).